

# Experimental and Monte Carlo simulation: the role of urea in mullite synthesis

G.P. Thim<sup>a,\*</sup>, C.A. Bertran<sup>b</sup>, V.E. Barlette<sup>b</sup>, M.I.F. Macêdo<sup>b</sup>, M.A.S. Oliveira<sup>a</sup>

<sup>a</sup>Chemistry Department, Instituto Tecnológico de Aeronáutica (ITA), Centro Técnico Aeroespacial, São José dos Campos, SP, Brazil

<sup>b</sup>Chemistry Institute, Universidade Estadual de Campinas (UNICAMP), SP, Brazil

Received 8 June 2000; received in revised form 22 August 2000; accepted 31 August 2000

## Abstract

Mullite was synthesized by a sol–gel process employing aqueous solution of silicic acid, aluminum nitrate and urea in high concentration (9 mol/l). t-Mullite crystallizes at temperatures around 1050°C, the fraction of the spinel phase formed was small and the apparent activation energy obtained by fitting the XRD results with the JMAK model was (770±4) kJ mol<sup>-1</sup>. Monte Carlo simulations were performed to investigate the site-site correlation function for ion (I)–urea (Ou) and ion (I)–water (Ow) interactions,  $g(r_{IOu})$  and  $g(r_{IOw})$ , respectively. The integration of these two correlation functions indicated the presence of four water and two urea molecules in the first Al<sup>3+</sup> coordination shell. The <sup>27</sup>Al nuclear magnetic resonance (NMR) results also indicate the presence of species like [Al(H<sub>2</sub>O)<sub>4</sub>(urea)<sub>2</sub>]<sup>3+</sup>. © 2001 Elsevier Science Ltd. All rights reserved.

**Keywords:** Monte Carlo methods; Mullite; Sol-gel processes; Urea

## 1. Introduction

Ceramic materials, such as mullite (3Al<sub>2</sub>O<sub>3</sub>·2SiO<sub>2</sub>), have been extensively studied due to their low thermal expansion, high creep resistance at elevated temperature, etc.<sup>1</sup> Mullite has been prepared by single phase gels and diphasic gels. Xerogels derived from single phase gels typically crystallize to mullite around 980°C, while colloidal gels crystallize at temperatures above 1250°C. This behavior for diphasic gels is attributed to local compositional inhomogeneities that lead to the formation of intermediate phase such as spinel or γ-alumina prior to mullite crystallization.<sup>2</sup> The crystallization temperatures vary with the homogeneity precursor degree.<sup>3–5</sup> The degree of homogeneity of aluminosilicate based materials precursors, prepared by sol–gel processes, depends on the starting materials, Al<sup>3+</sup> hydrolysis rate, and parameters associated to the drying and densification processes. Acetylacetone, carboxylates, carboxylic acids, and amides have been used to control the Al<sup>3+</sup> hydrolysis rate and the drying

process.<sup>6–8</sup> These species are chelating agents for the Al<sup>3+</sup> ion, reducing the fraction of hydrated aluminum ions in aqueous solution. Therefore, the rate of the olation and oxolation reactions is reduced by addition of these chelating agents to the reactant system. These agents also interfere in the drying process, acting as a dry chemical control agent (DCCA). They reduce the solvent interfacial tension effect upon the gel, avoiding the gel structure destruction and, also, the segregation of silica, aluminum oxide, or other aluminum species present in the gel.<sup>9,10</sup>

In previous work, we had observed that precursors of mullite, cordierite and alumina prepared with high urea concentration (9 mol/l) present a high degree of homogeneity.<sup>11–13</sup> The aim of this work was to study the role of urea during the mullite synthesis by a sol–gel process employing aqueous solution of silicic acid, aluminum nitrate and high urea concentration. Correlation between experimental results and computational simulation data was done. Optimized Potential for Liquid Simulation (OPLS) for water<sup>14</sup> and urea<sup>15</sup> were used to model interactions. Ion–solvent interactions were modeled by Coulombic and non Coulombic terms, between ion I and the solvent molecules (water/urea solution). Monte Carlo simulation data for the chemical interactions between Al<sup>3+</sup>(aq) and urea were related to <sup>27</sup>Al NMR

\* Corresponding author. Tel.: +55-12-347-5958; fax: +55-12-347-5958.

E-mail address: gilmar@ief.ita.cta.br (G.P. Thim).

(nuclear magnetic resonance) spectrum and X-ray diffraction (XRD) results.

## 2. Experimental

### 2.1. Mullite synthesis

Sodium metasilicate ( $\text{Na}_2\text{SiO}_3 \cdot 5\text{H}_2\text{O}$ ) aqueous solution, 20 w/o, was passed through a previously treated bed of solid ion exchange resin ( $\text{H}^+$  form). The eluted liquid presented a pH equal to 3.5 and its silicon concentration was determined by titration. Depending on the silicon concentration, solid aluminum nitrate and urea were added to the silicic acid aqueous solution in an amount to keep a molar ratio of Si:Al:urea equal to 1:3:9. The obtained sol was kept in repose until the gel formation. An optically translucent gel was obtained. Its specific weight was determined by picnometry and was found to be equal to 1.2 g/cm<sup>3</sup>. All chemicals were analytical grade (Merck). The ionic exchanger was the IR 120 from Rohm and Hass. The xerogel was prepared by heating the formed gel in an oven at 50°C for 20 days. Xerogels were taken to an oven initially stabilized at  $(1050 \pm 2)^\circ\text{C}$  for 50 h. Calcium fluoride, in an amount necessary to perform a concentration close to 25 w/o, was added to each sample, after its air cooling to the room temperature. It was used as an internal standard for X-ray diffraction powder (XRD) in order to quantify the fraction of mullite ( $\alpha$ ) formed. A calibration curve was utilized to determine the mullite fraction.<sup>16</sup>

### 2.2. Measurements procedures

#### 2.2.1. Liquid $^{27}\text{Al}$ NMR

Liquid  $^{27}\text{Al}$  NMR spectra were recorded at 78.2 MHz using a spectrometer (Bruker AC 300/P). Typical pulse widths were 18  $\mu\text{s}$  for  $^{27}\text{Al}$  with delays between pulses of 2 s. A total of 2010 scans were recorded for each  $^{27}\text{Al}$  NMR spectra. A 1.0 mol/l aluminum nitrate aqueous solution was used as standard reference to chemical shifts.

#### 2.3. X-ray diffraction analysis (XRD)

The powder X-ray diffraction patterns were obtained in a diffractometer (Shimadzu, model XRD 6000) at 2° per min, using  $\text{CuK}\alpha$  radiation.

#### 2.4. Numerical simulations

Monte Carlo simulations for a 0.1 mol/l of  $\text{Al}^{3+}$  dissolved in 9 mol/l urea aqueous solution (1.2 g/cm<sup>3</sup> specific weight) were performed according to established procedures. These procedures include Metropolis criterion, periodic boundary conditions and spherical cut-

off radius.<sup>17</sup> The simulations were performed under constant molecule number ( $N$ , 390), isobaric ( $p$ , 1 atm) and isothermal ( $T$ , 298.15 K) ensemble ( $\text{NpT}$ ) and using the Diadorm program.<sup>18</sup> The utilized concentration of urea and  $\text{Al}^{3+}$  ion in the precursor solution corresponds to a cubic simulation box containing one  $\text{Al}^{3+}$  ion plus 78 urea molecules and 312 water molecules. Ion–solvent interaction was modeled by Coulombic and non-Coulombic terms between ion I and site  $j$  of the solvent molecule  $i$ , separated by a distance  $r_{Ij}$ , according to Eq. (1).

$$V_{Ii} = \sum_j^i \left[ A_{Ij} \exp(-B_{Ij}r_{Ij}) - \frac{D_{Ij}}{r_{Ij}^6} - \frac{E_{Ij}}{r_{Ij}^8} - \frac{F_{Ij}}{r_{Ij}^{12}} + \frac{q_I q_j}{4\pi\epsilon_0 r_{Ij}} \right] \quad (1)$$

The partial charge +3 was attributed to  $q_I$  and the partial charges  $q_j$  were those of the OPLS potentials for water and urea. The set of parameters  $A_{Ij}$ – $F_{Ij}$  for ion–water and ion–urea interactions was empirically developed by Monte Carlo simulation. The non-Coulombic part of Eq. (1) was calculated considering the oxygen sites of the water molecules (Ow), the oxygen sites of the urea (Ou) molecules and the nitrogen sites of the urea (Nu) molecules. Since the main interest was the structural properties in regions close to the ion, corrections for long range interactions, beyond the solvent–solvent and ion–solvent interactions cut-off radii, were done only for non-Coulombic terms. Averages for the thermodynamic properties and the site–site distribution functions were carried out using a total of  $0.20 \times 10^7$  configurations, after discharging configurations post-equilibrium.

## 3. Results and discussion

Fig. 1 shows the t-mullite fraction,  $\alpha = 73$  (w/o), crystallized from the xerogel calcination at  $(1050 \pm 2)^\circ\text{C}$  for 50 h. This figure also shows that t-mullite was the majority phase. The  $\text{CaF}_2$  peaks showed in this figure are those of the internal standard added to mullite powder, after calcination step, which were used to determine the mullite fraction ( $\alpha$ ) crystallized.<sup>16</sup> The crystallization temperature is somewhat lower than those published for mullite synthesis by other sol–gel aqueous routes.

Several isothermals [ $(1020, 1050, 1065, 1080, 1100 \pm 2)^\circ\text{C}$ ] for mullite crystallization were obtained using XRD data. Each isothermal was fitted by the JMAK equation, in order to obtain the time ( $t_{0.5}$ ) for 50 (w/o) mullite fraction ( $\alpha$ ). The apparent activation energy was obtained from the  $t_{0.5}$  dependence with the temperature, which is described by Arrhenius equation. The value determined in this work was  $(770 \pm 4)$  kJ

$\text{mol}^{-1}$  and it is lower than most data reported in the literature for diphasic gels (around  $1000 \text{ kJ mol}^{-1}$ ).<sup>19</sup>

The t-mullite crystallization temperature ( $1050 \pm 2^\circ\text{C}$ ), the small fraction of spinel formed and the apparent

activation energy indicate a high homogeneity degree for the xerogels prepared in this work. They were interpreted in terms of the xerogel constitution, which is composed of a silica matrix containing  $\text{Al}^{3+}$ ,  $\text{NO}_3^-$  and urea.

Site-site correlation functions computed by Monte Carlo simulations for the ion-urea,  $g(r_{\text{IOu}})$ , and ion-water,  $g(r_{\text{IOW}})$ , interactions are shown in Fig. 2. In this figure, the two sharp peaks around  $2 \text{ \AA}$  and that broad ones around  $4$  and  $6 \text{ \AA}$  represent the water and urea distance distribution around the aluminum ion. Fig. 3 shows the coordination numbers between the ion ( $\text{Al}^{3+}$ ) and the oxygen sites of the water molecule ( $\text{Ow}$ ) and between the ion ( $\text{Al}^{3+}$ ) and the oxygen sites of the urea ( $\text{Ou}$ ) molecule. They were calculated by integrating  $g(r_{\text{IOW}})$  and  $g(r_{\text{IOu}})$  under each peak of Fig. 2, up to the first minimum. Fig. 3 indicates the presence of four water and two urea molecules in the first coordination shell of the  $\text{Al}^{3+}$  ion and another ion coordination pattern for urea and water in the outside shells. Therefore, urea still takes part in the ion coordination even in the outside shells. It could be interesting to compare these Monte Carlo simulation results with XANES results obtained previously for very homogeneous gels prepared by slow alkoxide hydrolysis routes. In both cases a hexacoordinated environmental for aluminum ion was detected and a local structural order beyond the first coordination sphere was encountered.<sup>20</sup>

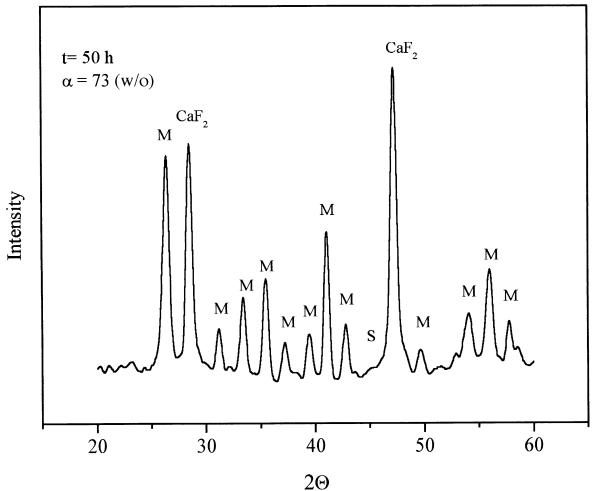


Fig. 1. XRD of the xerogel calcinated at  $(1050 \pm 2)^\circ\text{C}$ . M = mullite,  $\text{CaF}_2$  = calcium fluoride, S = spinel.

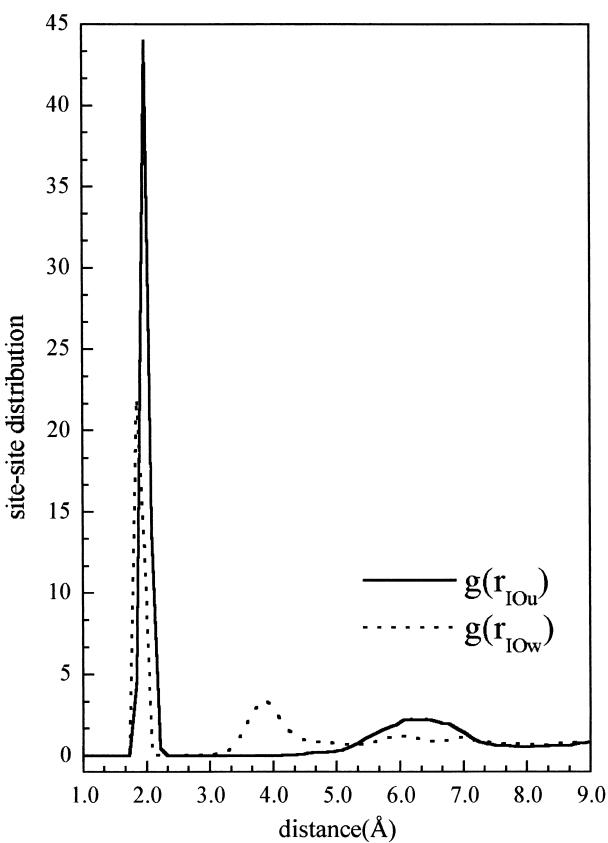


Fig. 2. Site-site correlation functions computed by Monte Carlo simulations for the ion-urea,  $g(r_{\text{IOu}})$ , and ion-water,  $g(r_{\text{IOW}})$ , interactions in 9 mol/l urea aqueous solutions at  $298.15 \text{ K}$  and 1 atm.

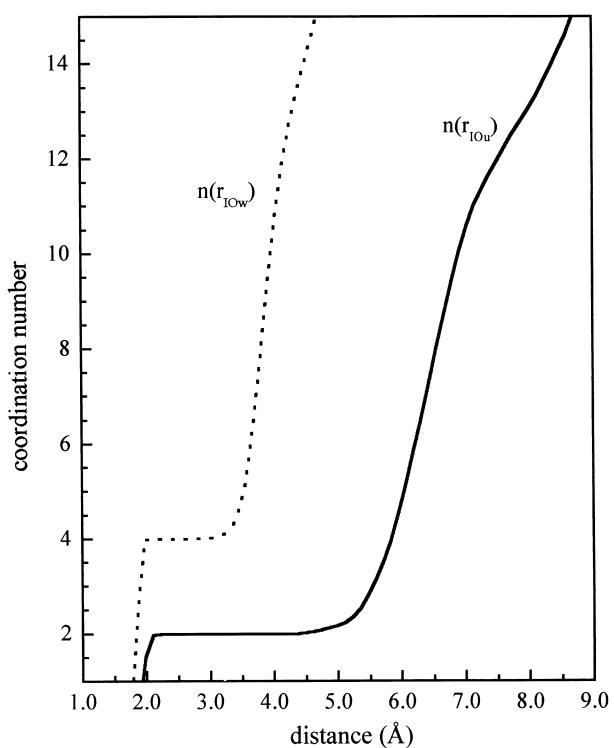


Fig. 3. Coordination numbers  $n(r_{\text{IOu}})$  and  $n(r_{\text{IOW}})$  at  $298.15 \text{ K}$  and 1 atm for 9 mol/l aqueous urea solutions.

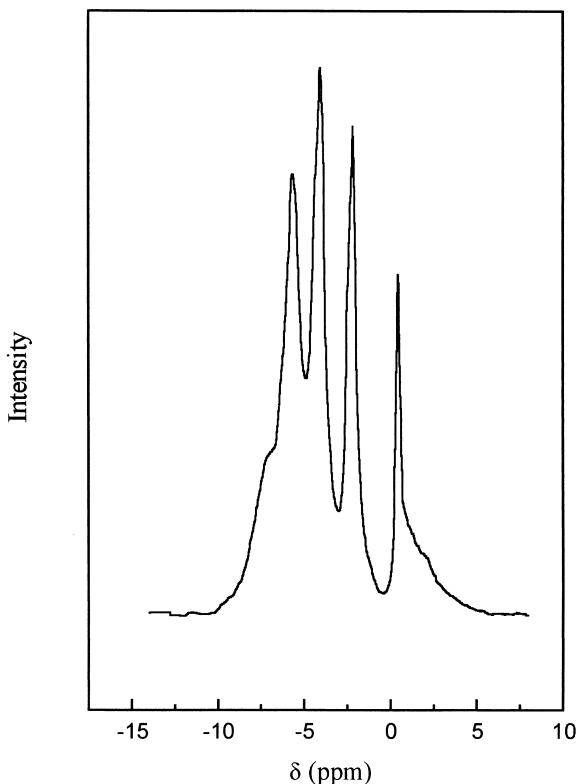


Fig. 4.  $^{27}\text{Al}$  NMR spectrum for an aqueous solution containing aluminum nitrate salt and urea in high concentration.

Fig. 4 shows the  $^{27}\text{Al}$  NMR spectrum for an aqueous solution containing aluminum nitrate salt and 9 mol/l urea concentration. The five peaks observed at 0.4, -2.3, -4.2, -5.8 and -7.4 ppm indicate the existence of five different types of solvated  $\text{Al}^{3+}$  ions. The peak at 0.4 ppm corresponds to the  $\text{Al}(\text{H}_2\text{O})_6^{3+}$  ion, which was utilized as a standard on the NMR spectrometer calibration. The peaks at -2.3 and -4.2 ppm were attributed by Wood<sup>21</sup> to  $[\text{Al}(\text{H}_2\text{O})_5(\text{urea})]^{3+}$  and  $[\text{Al}(\text{H}_2\text{O})_4(\text{urea})_2]^{3+}$  ions, respectively. The chemical specie  $[\text{Al}(\text{H}_2\text{O})_4(\text{urea})_2]^{3+}$  was predictable by the simulation performed in this work, while the specie  $[\text{Al}(\text{H}_2\text{O})_5(\text{urea})_1]^{3+}$  was not. As the  $\text{Al}^{27}$  NMR results and as the Monte Carlo simulation results indicate that urea takes part of the  $\text{Al}^{3+}$  coordination shell, with urea replacing water molecules in the ion solvation shell. Otherwise, urea should minimize the probability of segregation of the dispersed material in the silica matrix during the drying step, contributing for the higher homogeneity degree of mullite precursor, as observed.

#### 4. Conclusions

The xerogel prepared in this work, a silica matrix containing  $\text{Al}^{3+}$ ,  $\text{NO}_3^-$  and urea, presented a very high homogeneity degree. This high homogeneity was indi-

cated by the lower mullite crystallization temperature,  $(1050 \pm 2)^\circ\text{C}$ , low fraction of the spinel phase formed, and value of apparent activation energy<sup>-1</sup>. The integration of the site-site correlation functions, computed by Monte Carlo simulations, for ion-urea,  $g(r_{\text{IOu}})$ , and ion-water,  $g(r_{\text{IW}})$ , interactions, showed a coordination between the ion  $\text{Al}^{3+}$  and the oxygen sites of four water molecules ( $\text{Ou}$ ), and of two urea molecules ( $\text{Ou}$ ) in the first coordination shell of the  $\text{Al}^{3+}$  ion. These calculi also demonstrate an additional pattern for urea and water molecules in the outside shells. The  $^{27}\text{Al}$  NMR results indicated the existence of five different types of solvated  $\text{Al}^{3+}$  ions and the specie  $[\text{Al}(\text{H}_2\text{O})_4(\text{urea})_2]^{3+}$  was attributed to one of them. Therefore, both results, the Monte Carlo simulations and the  $^{27}\text{Al}$  NMR, indicate that urea takes part of the  $\text{Al}^{3+}$  coordination shell, with urea replacing the water molecules in the ion solvation shell.

#### Acknowledgements

The authors would like to thank CNPq and FAPESP for financial supports.

#### References

- Fahrenholz, W. G. and Smith, D. M., Effect of precursor particle size on the densification and crystallization behavior of mullite. *J. Am. Ceram. Soc.*, 1993, **76**(2), 433–437.
- Komarneni, S. and Roy, R., Mullite derived from diphasic nanocomposite gels. In *Ceramic Transactions, Vol. 6, Mullite and Mullite Matrix Composites*, ed. S. Somiya, R. F. Davis and J. A. Pask. American Ceramic Society, Westerville, OH, 1990, pp. 209–220.
- Yoldas, B. E., Effect of ultrastructure on crystallization of mullite. *J. Mater. Sci.*, 1992, **27**(24), 6667–6672.
- Barboux, P., Griesmar, P., Ribot, F. and Mazerolles, L., Homogeneity-related problems in solution derived powders. *J. Solid State Chem.*, 1995, **117**(2), 343–350.
- Yamawae, M., Aso, S., Okano, O. and Sakaino, T., Preparation of a gel from metal alkoxide and its properties as a precursor of oxide glass. *J. Mater. Sci.*, 1978, **13**, 865–870.
- Babonneau, F., Coury, L. and Livage, J., Aluminum sec-butoxide modified with ethyl acetoacetate—an attractive precursor for the sol-gel synthesis of ceramics. *J. Non-Cryst. Solids*, 1990, **121**, 153–157.
- Kansal, P. and Lame, R. M., A processable mullite precursor prepared by reacting silica and aluminum hydroxide with triethanolamine in ethylene glycol: structural evolution on pyrolysis. *J. Am. Ceram. Soc.*, 1997, **80**, 2597–2606.
- Pechini, M. *Method of Preparing Lead and Alkaline-Earth Titanates and Niobates and Coating Method Using the Same to Form a Capacitor*, US Patent 3,330,697, 1967.
- Ulrich, D. R., Prospects of sol-gel processes. *J. Non-Cryst. Solids*, 1988, **100**, 174–193.
- Boonstra, A. H., Bernardes, T. N. M. and Smits, J. J., The effect of formamide on silica sol-gel process. *J. Non-Cryst. Solids*, 1989, **109**(2–3), 141–152.
- Thim G. P., *Mullita: Sintese por Processamento Sol-gel*. PhD thesis, Chemistry Institute, UNICAMP, Campinas, SP, Brazil, 1997.

12. Lima, P. T., *Cordierita: Síntese por Processamento Sol-gel*. Master Dissertation, Chemistry Institute, UNICAMP, Campinas, Brazil, 1998.
13. Macêdo, M. I. F., *Síntese de Alumina por Processo Sol-gel: Cinética e Morfologia*. PhD thesis, Chemistry Institute, UNICAMP, Campinas, Brazil, 1999.
14. Jorgensen, W. L., Chandrasenkar, J., Madura, J. D., Impey, R. W. and Klein, M. L., Comparasion of simple potential functions for simulating liquid water. *J. Chem. Phys.*, 1983, **79**, 926–935.
15. Duffy, E. M., Severance, D. L. and Jorgensen, W. L., *Israel J. Chem.*, 1993, **33**, 323.
16. 16. Thim GP, Oliveira MAS, Bertran CA., Kinetic of mullite formation from inorganic precursors. In *Second International Latin-American Conference on Powder Technology*, 1999, p.28.
17. Allen, M. P. and Tildesley, D. J., *Computer Simulation of Liquids*. Clarendon, Oxford, 1987.
18. Freitas, L. C. G., *Diadorim Program, Version 2.0*. Departamento de Química, Universidade Federal de São Carlos, 1995.
19. Boccaccini, A. R., Khalil, T. K. and Bucker, M., Activation energy for the mullitization of a diphasic gel obtained from fumed silica and boehmite sol. *Mater. Lett.*, 1999, **38**(2), 116–120.
20. Colomban, P., Jones, D. J., Grandjean, D. and Flank, A.-M. *Journal of Non-Crystalline Solids*, 147–148, 135–140.
21. Wood, T. E., Sidle, A. R., Hill, J. R., Skarjure, R. P. and Goodbrake, C. J., *Mater. Res. Soc. Symp. Proc.*, 1990, **180**, 97.